



# Effect of adding a small amount of high molecular weight polyacrylamide on properties of oxidized cassava starch

Yan Liu<sup>a</sup>, Xu-chao Lv<sup>a</sup>, Xiao Hu<sup>a</sup>, Zhi-hua Shan<sup>b</sup>, Pu-xin Zhu<sup>a,\*</sup>

<sup>a</sup> Textile Institute, Sichuan University, Chengdu 610065, PR China

<sup>b</sup> Department of Leather, Sichuan University, Chengdu 610065, PR China

## ARTICLE INFO

### Article history:

Received 17 August 2009

Received in revised form 9 January 2010

Accepted 7 April 2010

Available online 14 April 2010

### Keywords:

Starch

Polyacrylamide

Polyvinyl alcohol

Mechanical property

Microstructure

Warp sizing

## ABSTRACT

Oxidized cassava starch (OCS) was blended with small proportions (0.5–3 wt%) of high molecular weight of a polyacrylamide (PAM) to overcome brittleness of the starch material for warp sizing. Properties of the starch-based sizes, blended with the PAM or polyvinyl alcohol (PVA), were compared in order to highlight the specific strengthening and toughening effects of the PAM on the OCS blends. The results showed that blending OCS with 3 wt% PAM resulted in growth of tensile strength and elongation at break by 25.67% and 51.59%, respectively. The viscosity stability and sizing performance were also enhanced. For equivalent performances of the starch sizes, the dosage of the PAM was needed only one-tenth of the PVA. Therefore, it was reasonable to expect a replacement of a large amount of PVA in a starch-based size by adding a small amount of the high molecular weight of PAM. The analyses of the phenomena by means of ATR–FTIR, SEM and XRD confirmed that hydrogen bonding interaction and chain entanglement occurred between PAM and OCS molecules, which could inhibit the crystallization of OCS and reduce the crystallite size in OCS/PAM blend films, and hence strengthen mechanical properties for the blends. While in the OCS/PVA blend, the two polymers had a tendency of self-crystallization, and PVA could increase the crystallite size of OCS and decrease its relative crystallinity.

© 2010 Elsevier Ltd. All rights reserved.

## 1. Introduction

Among various polymers available for textile sizes, starch has been considered as a good candidate because of its biodegradability, low price and abundant availability (Ma & Yu, 2004; Nakamura, Cordi, Almeida, Duran, & Mei, 2005). For the films made of starch alone, however, the semi-rigid characteristics of the molecular skeleton and strong intra- and inter-molecular hydrogen bonds result in brittleness (Ma & Yu, 2004) and poor processability of the films at low moisture content (Chen & Lai, 2008; Talja, Helén, Roos, & Joupplia, 2008; Yu, Wang, Wu, & Zhu, 2008). To overcome the shortcomings, starches and their derivatives are usually blended with various water-soluble polymers, especially with polyvinyl alcohol (PVA) for textile sizes (Jayasekara, Harding, Bowater, Christie, & Lonergan, 2004; Zhu, 2003). Nevertheless, PVA is needed in high mass ratio to starch in blends, sometimes as high as 1:1 (Lawton, 1996; Lee, Youn, Yun, & Yoon, 2007) or more, for improving the mechanical properties of starch sizes effectively. In the desizing process before textile dyeing and printing, the PVA desized remains in the desizing wastewater, which is not easy to be biodegraded comparing with biopolymers (Chiellini, Corti,

D'Antone, & Solaro, 2003; Lin & Lo, 1997) and is considered as an environmentally hazardous material (Ishigaki, Kawagoshi, Ike, & Fujita, 1999). Blends of starch with biodegradable polymers, one instance out of many is polyacrylamide (PAM) (Caulfield, Hao, Qiao, & Solomon, 2003; McAbee & Shomake, 1995), have generated particularly commercial interest. In textile industry, close attention has been paid to PAM as a substitute for PVA in starch-based sizes.

PAM has been used as a textile size owing to its good adhesion to fibers, compatibility with other sizes (El-Sayed, Abo-Shosha, & Ibrahim, 2009; Ibrahim, Hebeish, Fahmy, & Abo-Shosha, 2005), and film-forming performance (McAbee & Shomake, 1995). When mixed with starch or alone for warp sizing, PAM could provide the sized yarns with good mechanical properties and weavability (McAbee & Shomake, 1995; Moffett, 2000). A grafted copolymer of hydrolyzed starch with PAM was also used for size-based material, which could highly enhance mechanical properties of warp yarns with the good results originated from effectively chemical modification of PAM branched chains to the starch backbone (Mostafa, 1997).

PAM is a polymer of C–C linear backbone with an amide side group per construction unit, the long chains of which are easy to form a coiled structure and to entangle with each other in the solution (Shirota & Casrner, 2001). For the system of starch blended with PAM, the difference in the semi-rigid starch and flexible PAM polymers makes them difficult to achieve a composite with

\* Corresponding author. Tel.: +86 28 85405437; fax: +86 28 85405437.

E-mail address: [zhupxscu@163.com](mailto:zhupxscu@163.com) (P.-x. Zhu).

a desired level of molecular mixing, whereas the specific interactions like H-bonding (Ma & Yu, 2004) between the two polymers are favorable to their miscibility (He, Zhu, & Inoue, 2004). Introducing a polymer containing functional groups for hydrogen bonding into starch blends has been proven to be an effective method for improving the mechanical properties of a variety of starch blends, such as chitosan/starch (Xu, Kim, Hanna, & Nag, 2005), plasticized starch/polyurethane (Lu, Tighzert, Berzin, & Rondot, 2005), thermoplastic starch/polycaprolactone (Shin, Lee, Shin, Balakrishnan, & Narayan, 2004), and the like. On the other hand, the chain entanglement between components of polymer blends is relative to the molecular weight of the polymers involved, and linear polymers with high molecular weight undergo long range interactions (Carlsson & Jonsson, 1996) which plays a major role in improving the elongation at break (Chang, Ai, Chen, Dufresne, & Huang, 2008; Follain, Joly, Dole, & Bliard, 2005). From the two respects of miscibility and chain entanglement, it appears that the mechanical properties of starch may be modified by adding a high molecular weight PAM into the system in small quantities.

Based on these considerations mentioned above, a molecular weight of  $1.0 \times 10^7$  PAM was chosen to be blended in small amounts (0.5–3 wt%) with oxidized cassava starch (OCS) in the study, and the starch-based blends were prepared using cooking and casting method. The effects of the PAM on the viscosity, mechanical properties, and sizing performance of the OCS/PAM blend sizes were studied and compared with those of OCS/PVA blend sizes in large amounts (5–30 wt%) of PVA in order to highlight the specific strengthening and toughening effect of the PAM on OCS. Combined with the properties, the structural data obtained from ATR-FTIR, SEM and XRD were analyzed in order to get a basic understanding of the performance for the OCS/PAM blend sizes.

## 2. Experimental

### 2.1. Materials

Oxidized cassava starch (OCS) with 0.04 wt% carboxyl content was obtained from Sililun New Textile Co., Ltd. (Suining, China). Polyacrylamide (PAM) with molecular weight  $1.0 \times 10^7$  Da and anionicity ca. 1.5 mol% was from SNF, Inc. (Andrézieux Cedex, France; trade name: FLOPAM AH 912 SH). Polyvinyl alcohol (trade name: PVA 1799) was supplied by Sichuan Vinylon Co. Ltd. (Chongqing, China), and has been used extensively in warp sizing in China; it has an average DP 1700–1800 and an alcoholysis degree of  $99 \pm 1$  mol% with molecular weight of  $7.6 \times 10^4$ – $8.0 \times 10^4$  Da calculated from the DP and alcoholysis degree. Analytical grade  $\text{CuCl}_2$  was supplied by Kelong Chemical Reagent Co., Ltd. (Chengdu, China). Deionized water was used in all of the experiments.

### 2.2. Preparation of blend size pastes

OCS/PAM blend sizes were prepared as follows: a certain ratio of PAM and OCS powders was dispersed in deionized water with solid content 6 wt%, and then the system was heated from room temperature to the boiling point in a three-necked bottle in a thermostatic water bath and maintained in the boiling state for 1.5 h. The whole process was accompanied with constant stirring using a metal stirrer with 20.5 mm diameter at shear rate of 75 rpm. Contents of PAM in the blend compositions were 0%, 0.5%, 1%, 2%, and 3% (dry weight percentage), respectively.

OCS/PVA blend sizes were prepared by the same procedure as above, and PVA in their blend compositions were 5%, 10%, 15%, 20%, and 30% (dry weight percentage), respectively. These cooked blend sizes were for the preparation of blend films and for viscosity measurement.

### 2.3. Apparent viscosity determination of the pastes

Apparent viscosity of the blend pastes was measured with a rotating viscometer (trade name: NDJ-79; manufactured by Shanghai Ande Instrument Equipment Co., Ltd., Shanghai, China). The cooked pastes were cooled, while stirring, to 95 °C, 85 °C, 75 °C, 60 °C, 45 °C, 30 °C, respectively, and then the viscosity of the pastes was measured by using the 1# rotor of the viscometer at each temperature.

### 2.4. Film-forming of the blend sizes and mechanical properties measurement

Each of the cooked pastes in 60 ml volume was spread out with a syringe onto a 210 mm  $\times$  150 mm of glass dish paved with a polyester film of the same size, which rested on a leveled surface in ambient condition until the casting film was dried. The OCS/PAM or OCS/PVA blend films (about 0.1 mm thickness) were separated from the polyester film and equilibrated further in a desiccator with controlled RH 68% (over a saturated solution of  $\text{CuCl}_2$ ) at room temperature for three days.

As the blend films were equilibrated, the exact thickness of the films was measured using a centesimal thickness tester (trade name: CH-10-AT; made by Shanghai Liuling Instrument Co., Ltd., Shanghai, China). For every sample, ten data were recorded and the average thickness was taken. The tensile strength (TS) and elongation at break (E%) for blend films were determined using a tensile testing equipment (trade name: YG061; made by Laizhou Electron Instrument Co., Ltd., Laizhou, China) with a clamping distance of 100 mm and stretching speed of 100 mm/min. For each set of data, ten samples were tested, and the average values with the standard deviation were calculated.

### 2.5. Adhesiveness test

The sizing paste for the test was prepared by blending the PAM and the OCS in deionized water. The concentration of the sizing pastes on the basis of dry weight was fixed at 1%. The PAM in the OCS/PAM blends was 0%, 0.5%, 1%, 2%, and 3% (dry weight percentage), respectively, and the PVA in the OCS/PVA blends was 5%, 10%, 15%, 20%, and 30% (dry weight percentage), respectively. The resulting suspensions, volume 2500 ml each, were heated to the boiling point and maintained for 30 min, and then were placed into a thermostatic water bath maintained at 95 °C for use.

The cotton yarn and polyester spun yarn of loosely twisted slubbing were used for adhesiveness test by the impregnated roving method (Zhu & Chen, 2007). The yarns were encircled on a tailor-made metal rack, then the rack was dipped into the cooked paste at 95 °C and maintained for 5 min. After that, the sized yarns were hung to be dried at room temperature and equilibrated in a desiccator with controlled RH 68% (over a saturated solution of  $\text{CuCl}_2$ ) at room temperature for three days for evaluation.

The tensile strength (TS) of each sized yarns was determined using the YG061 Tensile Testing Equipment with a clamping distance of 100 mm and stretching speed of 100 mm/min. For each data point, 15 samples were tested, and the average values with its standard deviation were calculated.

### 2.6. Structure characterization

The film samples were cast using solutions of OCS, PAM and the OCS/PAM blend in a ratio of 1:1, respectively. FTIR spectra of the films were recorded by attenuated total reflection (ATR) method in FTS3000 FTIR Spectrum Scanner (Hercules, USA). After dried over  $\text{P}_2\text{O}_5$  powders, each film was allowed to contact intimately with the surface of the ATR crystal. The spectra data were collected over

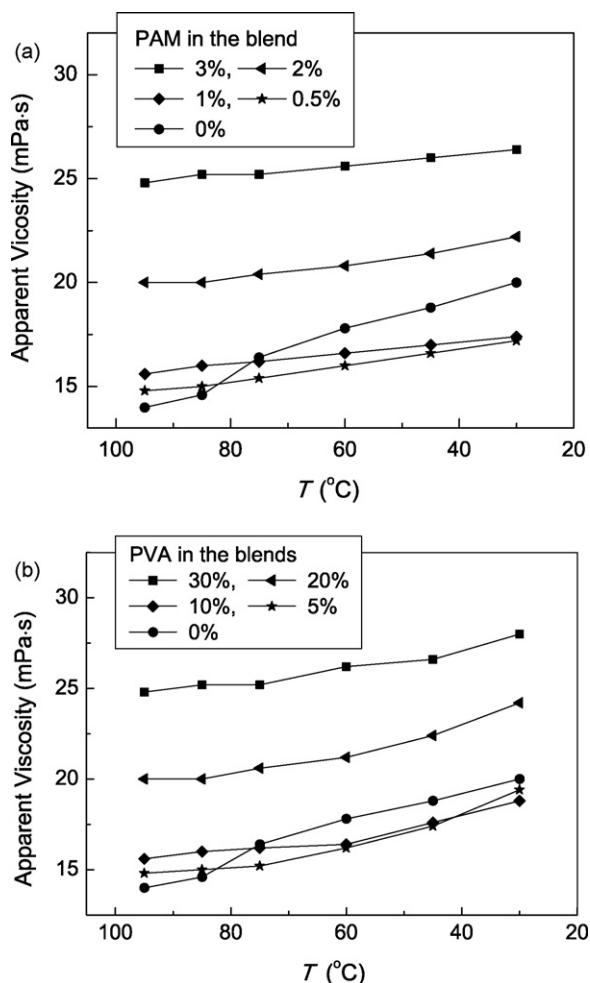


Fig. 1. Temperature dependence of apparent viscosity for (a) OCS/PAM and (b) OCS/PVA blend pastes. The solid content is 6 wt%.

32 consecutive scans with a resolution of  $4\text{ cm}^{-1}$  at room temperature.

SEM images were taken on a scanning electron microscope (Inspect F; FEI Company, Hillsboro, Oregon, USA). The film samples were sputtered with gold prior to the fractographic examination.

X-ray patterns of pure OCS film, PAM film and their composite films were analyzed using an X-ray diffractometer (XRD D/maxIIIa; Rigaku Co., Japan) with Cu radiation at a voltage of 40 kV and an electric current 30 mA. The samples were scanned between  $2\theta = 5\text{--}45^{\circ}$  with a scanning speed of  $0.5^{\circ}/\text{min}$ . Also, the films of PVA and OCS/PVA blends were scanned in the same way.

### 3. Results and discussion

#### 3.1. Apparent viscosity and viscosity stability

The viscosity of sizing liquor is a key factor affecting the sizing performance. In a sizing process for a given size composite and solid content, lower viscosity of the sizing paste always results in better fluid permeability, but worse coating property and lower add-on for the yarn. So, add-on and distribution uniformity of the size agents on the yarns depend to a large extent on the viscosity and stability of the sizing liquor. Fig. 1 showed the relationship of apparent viscosity dependence on temperature and the dosage of synthetic sizes in OCS/PAM and OCS/PVA blend sizes. It was found that there were significant rises of the viscosity of the OCS paste, as the temperature was decreased from  $85^{\circ}\text{C}$  to  $75^{\circ}\text{C}$ . This could be attributed to

Table 1

Comparison of tensile properties between OCS/PAM and OCS/PVA blend films.

Sample	Dosage (%)		Tensile strength (MPa)	Elongation at break (%)
	PAM	PVA		
OCS	–	–	$3.35 \pm 0.15$	$3.45 \pm 0.25$
OCS/PAM	0.5	–	$3.74 \pm 0.09$	$3.60 \pm 0.41$
	1	–	$4.05 \pm 0.20$	$4.29 \pm 0.85$
	2	–	$4.18 \pm 0.21$	$5.04 \pm 0.75$
	3	–	$4.21 \pm 0.23$	$5.23 \pm 0.69$
OCS/PVA	–	5	$3.43 \pm 0.12$	$3.49 \pm 0.29$
	–	10	$3.58 \pm 0.31$	$4.88 \pm 0.52$
	–	20	$3.77 \pm 0.25$	$5.16 \pm 0.55$
	–	30	$4.19 \pm 0.22$	$5.18 \pm 0.57$

the leached amylose molecules that interacted via H-bonding readily with each other, as temperature of the paste decreases, to form a rigid B-type double helices with a left-handed structure (Gidley, 1989) and a three-dimensional network (Putaux, Bulon, & Chanzy, 2000), which were referred to as quick setback or retrogradation of amylose in the paste. The same phenomenon of viscosity increase was observed in the work of Wang and Wang (2001) during cooling the pastes of acid-thinned corn, potato and rice starches at temperatures between  $85^{\circ}\text{C}$  and  $75^{\circ}\text{C}$  with an extent of rising viscosity corresponding positively to the amylose content.

As the PAM or PVA was added into the system, the paste viscosity increased greatly with increasing the content of synthetic polymers and increased slowly with decreasing temperature, but no significant viscosity rises for the blended pastes were observed from  $85^{\circ}\text{C}$  to  $75^{\circ}\text{C}$ , which could be attributed to some special interactions between amylose and the soluble synthetic polymers. In the sense of increasing the apparent viscosities, increasing PAM or PVA in the blends showed similar pictures reflected in Fig. 1(a) and (b). It should be noted that for any pairs of matched viscosity–temperature curves between Fig. 1(a) and (b), the dosage of PAM was only one-tenth of PVA in their respective starch-based blends. For example, in comparison with pure OCS paste at  $95^{\circ}\text{C}$  at which ordinary sizing processes implemented, the apparent viscosities of the blends with 3% PAM, Fig. 1(a), and with 30% PVA, Fig. 1(b), increased by about 77%. From a practical point of view, the viscosity behavior of OCS/PAM blend sizes in a small quantity of the PAM was substantially similar with that of OCS/PVA blend sizes in a large quantity of PVA under ordinary sizing conditions. Therefore, the similarity of the viscosity–temperature curves for the OCS/PAM and OCS/PVA blend sizes could lay a foundation for replacing a large amount of PVA in a starch-based size by adding a small amount of the high molecular weight of PAM.

H-bonding between amylose molecules results in an increase of paste viscosity as the system is cooling (Morris, 1990), i.e. short-term retrogradation. In Fig. 1 the viscosity uptrend for OCS/PAM was weak in comparison with the OCS paste. The phenomenon suggested that PAM interacted with starch via H-bonding, and thus hindered retrogradation of amylose. The effect was dependent on the molecular weight as well as interactions of the components. By comparison, PVA stabilized the paste viscosity at temperatures below  $60^{\circ}\text{C}$  in a lower efficiency than did PAM in their blended pastes; this resulted from lower molecular weight of PVA together with less interaction of PVA with starch in their blend paste (Zhu, 2003).

#### 3.2. Tensile properties

The tensile properties of the OCS/PAM and OCS/PVA blend films were given in Table 1. For OCS/PAM blend films, addition of PAM from 0.5% to 3% caused a significant increase in both TS and E%. Take the blend film with 3% PAM as an example, its TS and E% were

4.21 MPa and 5.23%, respectively, increasing by 25.67% and 51.59% over that of the pure OCS film. For OCS/PVA blend films similar enhancement behavior of tensile properties was observed, while the PVA was ten times as more dosage as PAM in the blends. As a result, adding a small amount of high molecular weight PAM could replace a large amount of PVA in starch-based sizes in the sense of equivalent tensile properties.

Previous studies (Bourtoom & Chinnan, 2008; Phan, Phan, Debeaufort, Voilley, & Luu, 2009) demonstrated that the hydrogen bonding between starch and other polymers can improve strength of the blend materials. Xia, Gao, Song, Zhang, and Zhang (2005) suggested that PAM and chitosan can form hydrogen bonding interaction, and these interaction points can act as physical cross-linking points to increase the chain entanglement, thus the chain movement of polyacrylamide is limited and the  $T_g$  of PAM is increased. As a result, the mechanical properties of the blend material are enhanced. Kausch and Dettenmaier (1982) presented that the ultimate strain and energy of fracture for glassy polymers strongly depend on the presence of entanglements. As the chains in blends reach a length longer than that of the critical molecular weight  $M_c$ , the molecules can form a coherently entangled physical network. In the light of above understanding, the phenomenon of the improved strength and toughness upon adding a small amount of high molecular weight PAM in the starch blends, in Table 1, could be due to the following reasons: entanglements between PAM and OCS chains were readily generated because of the long and flexible chains of PAM; and thus the moderately physical cross-linking mediated by the hydrogen bonding between PAM and OCS molecules facilitated the increase of the strength and elongation at break.

In view of the effect of molecular weight on entanglement, if a comparable molecular weight of PVA with the PAM used was available, it might perform as well as PAM, for the two of them are of hydrophilic nature and high molecular weight effect; but there might be another possibility that the PVA would be no match for the PAM in the sense of inter-molecular interactions. The discussion would be an interesting topic. It is pity that we cannot directly compare the PAM with PVA in this paper, because the molecular weight of PVA available commercially is only about  $1.3 \times 10^4$ – $1.3 \times 10^5$  (DP 300–3000), greatly lower than that of the PAM used in our experiments. In spite of that, we intend to analyze the differences of properties and structures between PVA and PAM in the OCS matrix later in the paper.

### 3.3. Adhesiveness

Adhesiveness of sizes to fibers would directly affect the quality and weaving performance of the sized yarns and the loom efficiency. In the study, the impregnated roving method (Zhu & Chen, 2007) was used to test the size adhesiveness, in which tensile strength (TS) of the roving sized by 1 wt % solution of size agents was tested to measure the adhesiveness of the size agents to the fibers. Fig. 2 showed the dependence of TS value on mass ratio of PAM or PVA in OCS-based blend sizes for polyester yarns and cotton yarns, respectively. The TS of yarns sized with OCS/PAM blend sizes increased more rapidly than that with OCS/PVA blend sizes as the mass ratio of synthetic polymers increased, which indicated a relatively higher strengthening effect of PAM. Furthermore, the TS values of roving yarns sized with OCS/PAM blends were approximately comparable with that of yarns sized with OCS/PVA blends, while the dosage of PAM was obviously less than that of PVA, even at levels as low as 10% of PVA. Therefore, the phenomenon that replacing a large amount of PVA by a small amount of high molecular weight of PAM in starch-based sizes could result in an equivalent sizing performance was observed again. The results may be from some special interactions between PAM and starch molecules, most probably via hydrogen bonding, which can improve interfa-

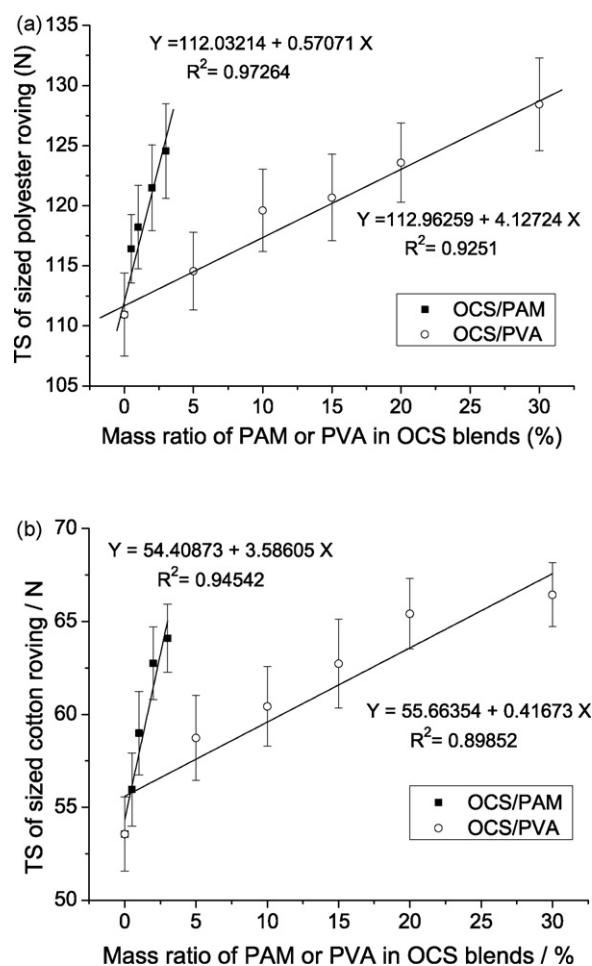


Fig. 2. Effect of mass ratio of PAM or PVA in OCS blend sizes on tensile strength of sized roving for (a) polyester yarns and (b) cotton yarns.

cial adhesion of polymeric blends (Massa, Shriner, Turner, & Voit, 1995).

### 3.4. FTIR spectroscopy

The ATR-FTIR technique was employed to verify the above-supposed hydrogen bonding interaction. Fig. 3 showed infrared spectra recorded at room temperature for OCS, PAM and OCS/PAM blend films in the  $1650$ – $1100$   $\text{cm}^{-1}$  region. For PAM the peak at  $1597$   $\text{cm}^{-1}$  was assigned to the bending vibration of N–H bond, which experienced a blue shift to  $1611$   $\text{cm}^{-1}$  as shown in the spectrum of OCS/PAM film, because of the H-bonding of PAM–N–H...O–OCS and an increase of the energy that the bending vibration needed. On the other hand for OCS, the peak  $1157$   $\text{cm}^{-1}$  had been attributed to C–O and C–C stretching (Dumoulin, Alex, Szabo, Cartilier, & Mateescu, 1998), which shifted to  $1150$   $\text{cm}^{-1}$  in the case of the OCS/PAM blend, indicating the bonds elongated by the H-bonding. Furthermore, Bernazzani, Peyyavula, Agarwal, and Tatikonda (2008) attributed the peak  $1121$   $\text{cm}^{-1}$  for the starch spectrum to the H-bonding between starch molecules, while the peak almost disappeared in the OCS/PAM spectrum. It is possible that the hydrogen bondings among starch molecules of themselves were hindered and replaced by that between starch and PAM, as PAM was introduced into the blend.

Previous study (Jayasekara et al., 2004) revealed that there is no obvious H-bonding interaction between PVA and starch in the cast-blended films, which was verified by XRD, FTIR and  $^{13}\text{C}$  NMR techniques. The differences in strength of H-bonding between



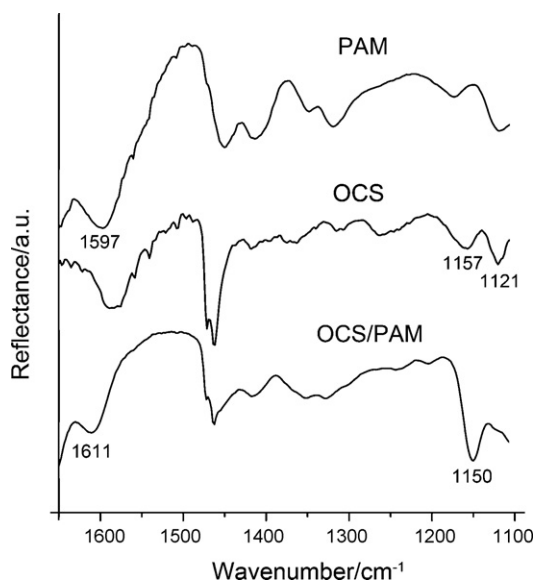


Fig. 3. FTIR-ATR spectra of OCS, OCS/PAM (1:1) and PAM films in the 1650–1100  $\text{cm}^{-1}$  region.

starch/PAM and starch/PVA may be resulted from relative strength of Lewis acid and base for the group pairs participated in forming the H-bonding. For example, H-bonding between acrylamino in PAM and hydroxy in starch will be stronger owing to hydrogen bond cooperativity than that between hydroxy pairs in the case of PVA–starch system and in starch of its own (Kuo & Chang, 2001).

### 3.5. Surface morphology of the films

Morphology studies can provide the information on miscibility of polymeric blends (Wang & Composto, 2003), so the surface morphology of the OCS film, OCS/PAM and OCS/PVA blend films was evaluated by SEM. The OCS film in Fig. 4(a) presented a coarse surface stacked by pelleted particles, which is believed to be resulted from amylopectin retrogradation (Lawton, 1996; Lopez-Rubio, Flanagan, Gilbert, & Gidley, 2008; Putaux et al., 2000; Xiong, Tang, Tang, & Zou, 2008), cocrystallization between amylose and amylopectin and from crystallization of amylopectin (Rindlav-Westling, Stading, & Gatenholm, 2002). The particle size became smaller with adding PAM in a pattern that seemed to prevent the particles from growing, and a more uniform and smooth surface was observed; this suggested that determinate miscibility existed between PAM and OCS. Similar observations were reported for other starch blend films, which had been attributed to strong hydrogen bonding between starch and other components (Phan et al., 2009; Wu, Geng, Chang, Yu, & Ma, 2009; Xiong et al., 2008). When the SEM photos were magnified, we can see from Fig. 4(a) that the maximum diameter of the pellets was dramatically reduced with increase of PAM content, e.g. from ca. 2  $\mu\text{m}$  for OCS film to ca. 0.5  $\mu\text{m}$  for OCS/PAM blend film with 2% PAM.

OCS/PVA films, however, as seen in Fig. 4(b), presented a “sea-island” structure on the surface with the particle size of ca. 4  $\mu\text{m}$ , even much coarser than the pure OCS film; this indicated that a phase separation occurred during the film forming. Furthermore, the aggregated particles did not decrease their pellet size but their aggregation number decreased with increasing PVA content, as if the island melt bit by bit into the sea, which was not observed in OCS/PAM blend films possibly owing to miscibility of OCS and PAM molecules. Similarly, Jayasekara et al. (2004) revealed a starch/PVA cast film flexible and homogeneous on a macroscopic scale but on a microscopic scale there seemed to be small patches of individ-

ual components. Zhu (2003) showed another evidence of phase separation for the starch/PVA system in paste.

### 3.6. Crystallization analysis

Crystallization of starch materials is of great technological importance due to the effect on their mechanical properties. In view of that, the influence of PAM or PVA on crystallization of the OCS was investigated by use of X-ray diffraction patterns for the films, shown in Fig. 5, together with their crystallographic data on some crystal planes in Table 2.

As shown in Fig. 5(a), a total amorphous pattern was clearly observed for the PAM film, while the OCS film had four main diffraction peaks appearing at  $2\theta = 5.5^\circ$ ,  $17.1^\circ$ ,  $19.6^\circ$  and  $22.3^\circ$ , respectively, corresponding to the crystalline feature of a typical B-type hexagonal unit cell crystalline structure (Wang, Yu, & Yu, 2008). The characteristic diffraction peaks of B-type crystal of the OCS kept almost the same position regardless of contents of the PAM, but the XRD intensity varied. The peak at  $2\theta = 17.1^\circ$  corresponding to  $\{1\ 2\ 1\}$  crystal plane (Lopez-Rubio et al., 2008) became dominant and sharp. In order to quantitatively analyze crystallization behavior of the OCS film and OCS/PAM blend films with various PAM contents, the total crystallinity (TC), relative crystallinity (RC), the dimension of the unit cell (DUC) and the crystallite size (CS) at  $2\theta = 17.1^\circ$  on  $\{1\ 2\ 1\}$  plane were calculated by MDI Jade 5.0 software and presented in Table 2. It was found that the TC value gradually decreased from 9.15% for OCS to 5.70% for the blend film with 3% PAM, together with decrease of crystallite size from 95 Å to 74 Å on the  $\{1\ 2\ 1\}$  plane, the tendency of which was in agreement with the phenomena observed in Fig. 4(a) for the blend films. Because of miscibility that the blend films displayed by SEM and FTIR, the OCS spherulites became smaller and finely distributed. The X-ray data clearly indicated that amylopectin retrogradation in the films was inhibited by PAM. In addition, with increasing PAM content, the dimension of the unit cell at  $2\theta = 17.1^\circ$  increased (Table 2); this indicated that PAM might participate in or affect crystallization of OCS via H-bonding verified by the analysis of ATR-FTIR (Fig. 3). As a result of miscibility and chain entanglements of the PAM and OCS, the physical cross-linking would increase the friction among the molecular chains, lower the mobility of the starch chains to the front of crystal growth, and then hinder the starch from spherulite growth.

Generally, imperfect crystals containing defects are typical of a brittle matrix, whereas perfect crystals may contribute to the improved toughness (Wong, Shanks, & Hodzic, 2004). It is obvious that a fine distribution of crystal particles in semicrystalline polymers can reduce the inner stress concentration in the material, which in turn leads to an extensive shear deformation. By way of incorporation of the long chain PAM into the OCS, such factors as the hydrogen bonding interaction that could enhance the tensile strength by interfacial adhesion in polymeric blends (Massa et al., 1995), the relatively perfect crystal spherulites that could result in toughening effect, and chain entanglements that could act as physical cross-linking points between PAM and OCS to form a network in the matrix structure, were considered to be responsible for enhancing and toughening the OCS/PAM blend film, as well as for steadying properties of the blend pastes.

By comparison, PVA exhibited a semicrystalline structure, as shown in Fig. 5(b), with the peak at  $2\theta = 19.7^\circ$  corresponding to  $\{1\ 0\ 1\}$  crystal plane (Strawhecker & Manias, 2000) as seen in Table 2, where the total crystallinity (TC), the relative crystallinity (RC), the dimension of the unit cell (DUC) and the crystallite size (CS) at  $2\theta = 19.7^\circ$  and  $2\theta = 17.1^\circ$  were calculated by use of MDI Jade 5.0 software, respectively. There were four reasoned thinkings from the data in Table 2: (A) TC increased with increasing PVA content, which was on the whole attributed to crystallization of PVA

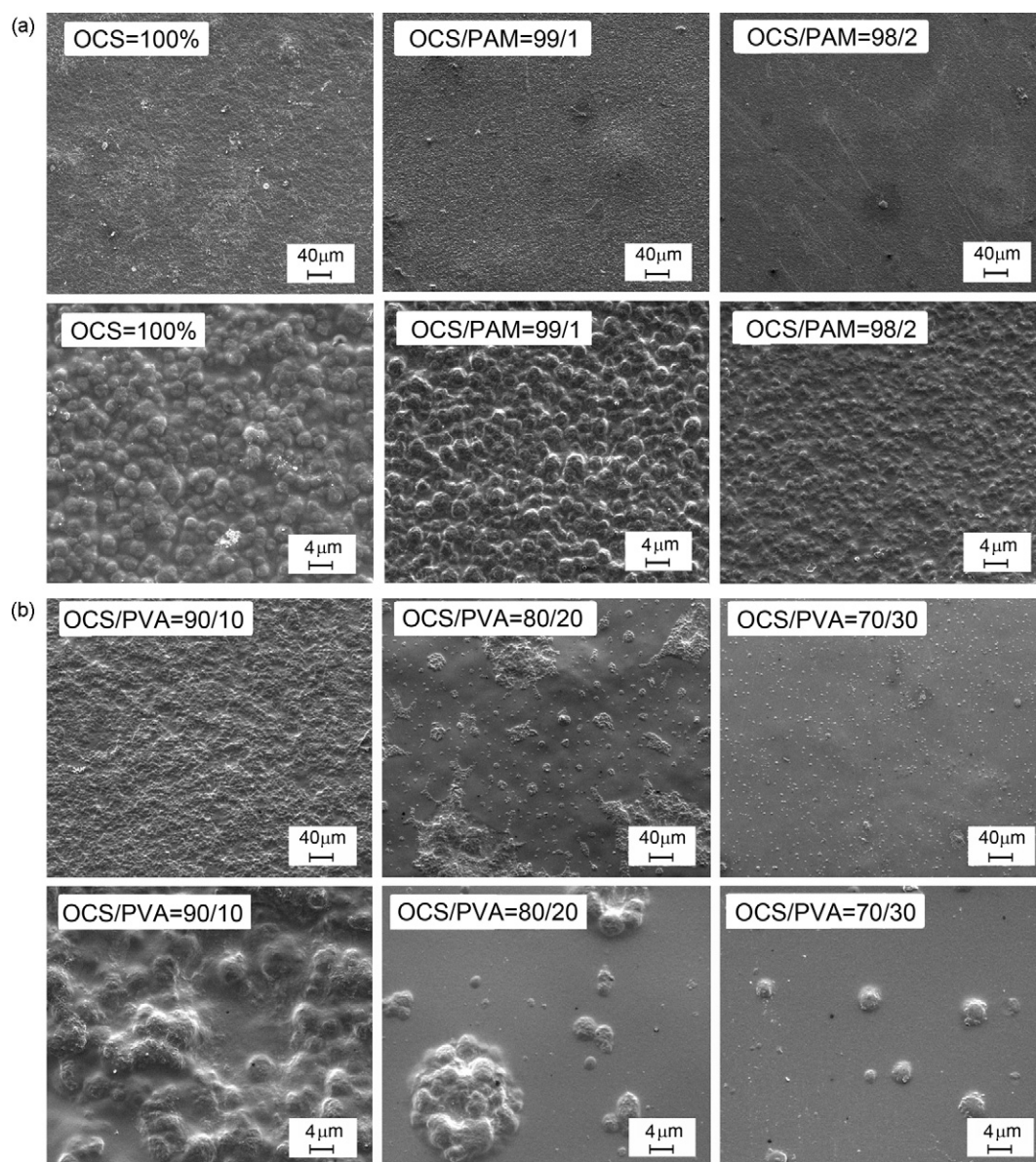


**Fig. 4.** SEM images of (a) the OCS film and the OCS blend films with 1 and 2 wt% PAM, and (b) the OCS blend films with 10 wt%, 20 wt% and 30 wt% PVA.

reflected from RC at  $2\theta = 19.7^\circ$  and responsible for enhanced tensile properties (Table 1). (B) For  $2\theta = 17.1^\circ$  relative to OCS crystallinity, RC decreased but the CS increased with increasing PVA content, which was in accordance with SEM observations (Fig. 4(b)). (C) Also for  $2\theta = 17.1^\circ$ , the DUC of the starch remained unchanged as

PVA content increased, which indicated no PVA molecules to participate in crystallization of starch. In this case, PVA would take the conformation either to be crystallized itself or to be associated with starch in amorphous region. And (D) with increasing PVA content, the RC of the OCS dramatically decreased and the RC of the PVA

**Table 2**

Total crystallinity (TC), relative crystallinity (RC), dimension of unit cell (DUC) and crystallite size (CS) of films for pure OCS, pure PVA, OCS/PAM and OCS/PVA blends.

Sample	Dosage (%)		TC (%)	RC (%)		DUC (Å)		CS (Å)	
	PAM	PVA		$2\theta$		$2\theta$		$2\theta$	
				17.1°	19.7°	17.1°	19.7°	17.1°	19.7°
OCS	–	–	9.15	7.14	–	5.17	–	95	–
OCS/PAM	1	–	7.50	5.56	–	5.18	–	83	–
	2	–	5.72	4.30	–	5.19	–	76	–
	3	–	5.70	4.21	–	5.20	–	74	–
OCS/PVA	–	10	11.05	6.17	3.29	5.17	4.46	98	93
	–	20	17.46	2.35	12.15	5.17	4.55	112	94
	–	30	20.29	0.8	18.64	5.17	4.51	115	94
	–	100	27.67	–	27.56	–	4.58	–	94

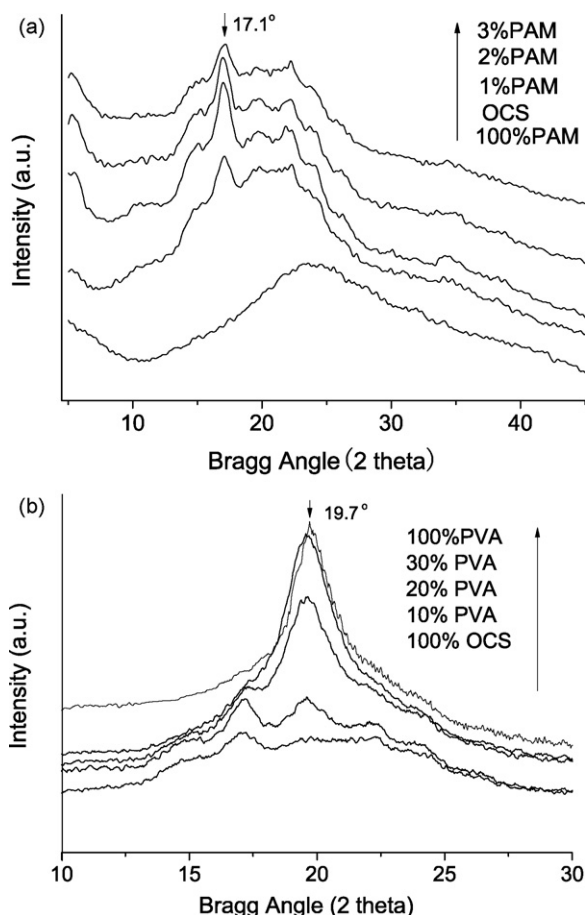


Fig. 5. Wide-angle XRD patterns of (a) pure PAM, pure OCS and OCS/PAM blend films with varied concentrations of PAM, and (b) pure PVA, pure OCS and OCS/PVA blend films with varied concentrations of PVA.

contrarily increased, and upon a certain amount of PVA added into the OCS/PVA blend, for example 30% PVA in our experiment, almost no crystallite character of OCS could be observed.

Arithmetic averages of the total crystallinity (TC) for OCS/PVA blends with PVA 10%, 20% and 30%, calculated from TCs of the pure OCS (9.15%) and pure PVA (27.67%), were 11.00%, 12.85% and 14.71%, respectively, comparing with the TC values from XRD data of 11.05%, 17.46% and 20.29% in Table 2. The difference and variation tendency depended on the PVA content in the blend. As the ratio of PVA added was small, e.g. 10% PVA, the TC from XRD data was about equal to the arithmetic average, which suggested no special interactions between the two components and reflected a macroscopic phase separation structure of individual components. As PVA content increased, TCs in Table 2 tended to be higher than the arithmetic average, which implied that the OCS could induce crystallization of PVA which may be a representative of microscopic phase separation where the PVA crystals separated from OCS/PVA blend in amorphous state.

The results and discussion above along with SEM observations suggested a picture that in the OCS/PVA system a small ratio of PVA would promote crystal growth of OCS with a macroscopic phase separation; and in the case of large ratios of PVA mixed, PVA would crystallize itself with a tendency of becoming microscopic phase separation from OCS/PVA amorphous matrix. Although more studies are needed to confirm the mechanism, such affirmation can be drawn as that in addition of PVA the OCS could increase its crystallite size as a result of phase separation, especially evident when a small ratio of PVA added. This was different from the case of OCS/PAM system where PAM decreased the relative crystallinity

and crystallite size of the OCS. This can also be used to argue that if a comparable molecular weight of PVA with the PAM used was available, it might not perform as well as the PAM, in the sense that PAM is an amorphous polymer with better H-bonding ability to interact with starch molecule, while PVA is a semicrystalline polymer with poor interaction with starch. This together with entanglement effect also explains why adding a small amount of high molecular weight PAM into the OCS material exhibits an increased mechanical behavior.

#### 4. Conclusions

In the paper, a high molecular weight of PAM were used in weight percent of 0.5–3% in OCS/PAM blends, to replace PVA 5–30% by weight in OCS/PVA blended textile sizes. Such the sizing properties of the OCS/PAM blends, as paste viscosity and its stability at lower temperature, tensile performance of the blend films, and adhesiveness of the blends on cotton and on polyester fibers, could substantially match with the OCS/PVA blends, and yet the dosage of PAM was only one-tenth of PVA to get roughly equivalent performances. Microstructural analyses confirmed the hydrogen bonding interaction and the chain entanglement between the amorphous PAM and OCS, and finely distributed spherulites and relatively perfect crystals for the OCS/PAM blend films, which were responsible for the enhanced sizing performance, and tensile and toughening effects. In contrast, adding the semicrystalline PVA into OCS led to a larger crystallite size and decreased relative crystallinity of OCS. Small ratios of PVA led to a macroscopic phase separation and a crystal growth of OCS in the OCS/PVA system; and large ratios of PVA were favorable to crystallization of PVA with a tendency of becoming microscopic phase separation from OCS/PVA amorphous matrix. Therefore, OCS/PVA blends with larger proportion of PVA had a good sizing performance. In other words, increase of mechanical properties for OCS/PVA blends was due to the presence of PVA. In summary, the PAM did provide the OCS size agent with better sizing behavior. So it was reasonable to expect that small amounts of high molecular weight of PAM could replace large amounts of PVA in starch-based sizes.

#### Acknowledgements

The authors thank the National High-tech R&D Program of China (Grand No. 2007AA03Z344), the Chinese Natural Science Foundation (Grant No. 50673062) and the Cooperation Project of Guangdong Province and Ministry of Education of China (Grant No. 2008B090500107) for their financial supports.

#### References

- Bernazzani, P., Peyyavula, V. K., Agarwal, S., & Tatikonda, R. K. (2008). Evaluation of the phase composition of amylose by FTIR and isothermal immersion heats. *Polymer*, 49(19), 4150–4158.
- Bourtoom, T., & Chinnan, M. S. (2008). Preparation and properties of rice starch-chitosan blend biodegradable film. *LWT-Food Science and Technology*, 41(9), 1633–1641.
- Carlsson, C., & Jonsson, M. (1996). Spectroscopic study of orientation dynamics of DNA during electrophoresis in entangled and dilute polyacrylamide solutions. *Macromolecules*, 29(24), 7802–7812.
- Caulfield, M. J., Hao, X. J., Qiao, G. G., & Solomon, D. H. (2003). Degradation on polyacrylamides. Part I. Linear polyacrylamide. *Polymer*, 44, 1331–1337.
- Chang, P. R., Ai, F., Chen, Y., Dufresne, A., & Huang, J. (2008). Effects of starch nanocrystal-graft-polycaprolactone on mechanical properties of waterborne polyurethane-based nanocomposites. *Journal of Applied Polymer Science*, 111(2), 619–627.
- Chen, C. H., & Lai, L. S. (2008). Mechanical and water vapour barrier properties of tapioca starch/decolorized hsian-tsao leaf gum films in the presence of plasticizer. *Food Hydrocolloids*, 22, 1584–1595.
- Chiellini, E., Corti, A., D'Antone, S., & Solaro, R. (2003). Biodegradation of poly(vinyl alcohol) based materials. *Progress in Polymer Science*, 28, 963–1014.



- Dumoulin, Y., Alex, S., Szabo, P., Cartilier, L., & Mateescu, M. A. (1998). Cross-linked amylose as matrix for drug controlled release. X-ray and FT-IR structural analysis. *Carbohydrate Polymers*, 37, 361–370.
- El-Sayed, Z. M., Abo-Shosha, M. H., & Ibrahim, N. A. (2009). Preparation of polyethylene glycol/polyacrylamide adduct and utilization in cotton finishing. *Carbohydrate Polymers*, 75, 479–483.
- Follain, N., Joly, C., Dole, P., & Bliard, C. (2005). Properties of starch based blends. Part 2. Influence of poly vinyl alcohol addition and photocrosslinking on starch based materials mechanical properties. *Carbohydrate Polymers*, 60, 185–192.
- Gidley, M. J. (1989). Molecular mechanisms underlying amylose aggregation and gelation. *Macromolecules*, 22, 351–358.
- He, Y., Zhu, B., & Inoue, Y. (2004). Hydrogen bonds in polymer blends. *Progress in Polymer Science*, 29, 1021–1051.
- Ibrahim, N. A., Hebeish, A., Fahmy, H. M., & Abo-Shosha, M. H. (2005). Synthesis characterization and application of poly(acrylamide)/poly(vinyl alcohol) polyblends. In *2nd international conference of textile research division (textile processing: state of the art and future developments)* NRC, Cairo, (pp. 11–13).
- Ishigaki, T., Kawagoshi, Y., Ike, M., & Fujita, M. (1999). Biodegradation of a polyvinyl alcohol-starch blend plastic film. *World Journal of Microbiology and Biotechnology*, 15, 321–327.
- Jayasekara, R., Harding, I., Bowater, I., Christie, G. B. Y., & Lonergan, G. T. (2004). Preparation, surface modification and characterization of solution cast starch PVA blended films. *Polymer Testing*, 23, 17–27.
- Kausch, H. H., & Dettenmaier, M. (1982). On some mechanical effects in glassy polymers attributed to chain entanglements. *Colloid and Polymer Science*, 260, 120–123.
- Kuo, S. W., & Chang, F. C. (2001). Studies of miscibility behavior and hydrogen bonding in blends of poly(vinylphenol) and poly(vinylpyrrolidone). *Macromolecules*, 34, 5224–5228.
- Lawton, J. W. (1996). Effect of starch type on the properties of starch containing films. *Carbohydrate Polymers*, 29, 203–208.
- Lee, W. J., Youn, Y. N., Yun, Y. H., & Yoon, S. D. (2007). Physical properties of chemically modified starch (RS4)/PVA blend films—Part 1. *Journal of Polymers and the Environment*, 15, 35–42.
- Lin, S. H., & Lo, C. C. (1997). Fenton process for treatment of desizing wastewater. *Water Research*, 31(8), 2050–2056.
- Lopez-Rubio, A., Flanagan, B. M., Gilbert, E. P., & Gidley, M. J. (2008). A novel approach for calculating starch crystallinity and its correlation with double helix content: A combined XRD and NMR study. *Biopolymers*, 89(9), 761–768.
- Lu, Y., Tighzert, L., Berzin, F., & Rondot, S. (2005). Innovative plasticized starch films modified with waterborne polyurethane from renewable resources. *Carbohydrate Polymers*, 61, 174–182.
- Ma, X. F., & Yu, J. G. (2004). The plasticizers containing amide groups for thermoplastic starch. *Carbohydrate Polymers*, 57, 197–203.
- Massa, D. J., Shriner, K. A., Turner, S. R., & Voit, B. I. (1995). Novel blends of hyperbranched polyesters and linear polymers. *Macromolecules*, 28, 3214–3220.
- McAbee, M. L., & Shomake, D. H. (1995). Process for sizing spun yarns. *US Patent Office*, Pat. No. 5,397,633.
- Moffett, R. H. (2000). Modified starch composition for removing particles from aqueous dispersions. *US Patent Office*, Pat. No. 6,048,929.
- Morris, V. J. (1990). Starch gelation and retrogradation. *Trends in Food Science and Technology*, 1(1), 2–6.
- Mostafa, Kh. M. (1997). Synthesis of poly(acryl amide)-starch and hydrolyzed starch graft copolymers as a size base material for cotton textiles. *Polymer Degradation and Solubility*, 55, 125–130.
- Nakamura, E. M., Cordi, L., Almeida, G. S. G., Duran, N., & Mei, L. H. I. (2005). Study and development of LDPE/starch partially biodegradable compounds. *Journal of Materials Processing Technology*, 162–163, 236–241.
- Phan, T. D., Phan, T., Debeaufort, F., Voilley, A., & Luu, D. (2009). Biopolymer interactions affect the functional properties of edible films based on agar, cassava starch and arabinoxylan blends. *Journal of Food Engineering*, 90(4), 548–558.
- Putaux, J. L., Bulon, A., & Chanzy, H. (2000). Network formation in dilute amylose and amylopectin studied by TEM. *Macromolecules*, 33(17), 6416–6422.
- Rindlav-Westling, Å., Stading, M., & Gatenholm, P. (2002). Crystallinity and morphology in films of starch. Amylose and amylopectin blends. *Biomacromolecules*, 3, 84–91.
- Shin, B. Y., Lee, S. I., Shin, Y. S., Balakrishnan, S., & Narayan, R. (2004). Rheological, mechanical and biodegradation studies on blends of thermoplastic starch and polycaprolactone. *Polymer Engineering and Science*, 44, 1429–1438.
- Shirot, H., & Casrner, E. W. (2001). Ultrafast dynamics in aqueous polyacrylamide solutions. *The Journal of the American Chemical Society*, 123(51), 12877–12885.
- Strawhecker, K. E., & Manias, E. (2000). Structure and properties of poly(vinyl alcohol)/Na<sup>+</sup> montmorillonite nanocomposites. *Chemistry of Materials*, 12, 2943–2949.
- Talja, R. A., Helén, H., Roos, Y. H., & Joupplia, K. (2008). Effect of type and content of binary polyol mixtures on physical and mechanical properties of starch-based edible films. *Carbohydrate Polymers*, 71, 269–276.
- Wang, H., & Composto, R. J. (2003). Wetting and phase separation in polymer blend films: Identification of four thickness regimes with distinct morphological pathways. *Interface Science*, 11, 237–248.
- Wang, L., & Wang, Y. (2001). Structures and physicochemical properties of acid-thinned corn, potato and rice starches. *Starch [Stärke]*, 53, 570–576.
- Wang, S. J., Yu, J. L., & Yu, J. G. (2008). Conformation and location of amorphous and semi-crystalline regions in C-type starch granules revealed by SEM, NMR and XRD. *Food Chemistry*, 110, 39–46.
- Wong, S., Shanks, R. A., & Hodzic, A. (2004). Mechanical behavior and fracture toughness of poly(L-lactic acid)-natural fiber composites modified with hyperbranched polymers. *Macromolecular Materials and Engineering*, 289, 447–456.
- Wu, Y., Geng, F. Y., Chang, P. R., Yu, J. G., & Ma, X. F. (2009). Effect of agar on the microstructure and performance of potato starch film. *Carbohydrate Polymers*, 76(2), 299–304.
- Xia, Y. Q., Gao, T. Y., Song, M. D., Zhang, B. H., & Zhang, B. L. (2005). Hemoglobin recognition by imprinting in semi-interpenetrating polymer network hydrogel based on polyacrylamide and chitosan. *Biomacromolecules*, 6(5), 2601–2606.
- Xiong, H. G., Tang, S. W., Tang, H. L., & Zou, P. (2008). The structure and properties of a starch-based biodegradable film. *Carbohydrate Polymers*, 71(2), 263–268.
- Xu, Y. X., Kim, K. M., Hanna, M. A., & Nag, D. (2005). Chitosan-starch composite film: Preparation and characterization. *Industrial Crops and Products*, 21, 185–192.
- Yu, J. H., Wang, J. L., Wu, X., & Zhu, P. X. (2008). Effect of glycerol on water vapor sorption and mechanical properties of starch/clay composite films. *Starch [Stärke]*, 60, 257–262.
- Zhu, Z. F. (2003). Starch mono-phosphorylation for enhancing the stability of starch/PVA blend pastes for warp sizing. *Carbohydrate Polymers*, 54, 115–118.
- Zhu, Z. F., & Chen, P. H. (2007). Carbamoyl ethylation of starch for enhancing the adhesion capacity to fibers. *Journal of Applied Polymer Science*, 106(4), 2763–2768.

**Yan Liu** is a master's degree student in textile chemistry and dyeing and finishing engineering at Sichuan University, China. She is engaged in researches involving polymer blends and modified starch applied in textiles.

**Xu-chao Lv** is a master's degree student in materials science at Sichuan University, China. He is engaged in researches involving polymer materials and modified starch blends.

**Xiao Hu** is a master's degree student in textile chemistry and dyeing and finishing engineering at Sichuan University, China. She is engaged in researches involving modified starch and textile auxiliary materials.

**Zhi-hua Shan** is a professor at Department of Leather, Sichuan University, China. He received his PhD in leather chemistry and engineering from Sichuan University in 1997. His research interests include physical chemistry, tanning technology, biomass chemical engineering, and leather chemicals.

**Pu-xin Zhu** is a professor at the Textile Institute, Sichuan University, China. He received his PhD in materials science from Sichuan University in 2001. His research interests include polymers, surface chemistry, nanocomposites, and textile sizes.